

Experimental Study and Prediction Model for Flexural Behaviour of Reinforced SCC Beam Containing Steel Fibers

Xiliang Ning^a, Yining Ding^a, Fasheng Zhang^b, Yulin Zhang^c

^a State Key Laboratory of Coastal and Offshore Engineering, Dalian University of Technology, Dalian 116023, China

^b China State Construction Technical Center, Beijing 101300, China

^c Center of Mathematics, University of Minho, Braga 4700-052, Portugal

Abstract: Seven full-scale steel fiber reinforced self-consolidating concrete (SFRSCC) beams were tested to study the effects of macro steel fibers on the flexural behaviour of reinforced self-consolidating concrete beams. The major test variables are fiber contents and longitudinal reinforcement ratios. The ultimate load, midspan deflections, steel reinforcement strains, crack width and crack spacing were investigated. The enhanced ultimate flexural capacity and reduced midspan deflection due to the addition of steel fibers were observed. With the increasing of fiber contents, the strain in longitudinal reinforcement, crack width and crack spacing decreased significantly. The possibility of using steel fibers for partial replacement of the conventional longitudinal reinforcement is estimated, which is meaningful for extending the structural application of SFRSCC. A method incorporating fiber contribution to the post-cracking tensile strength of concrete in the flexural analysis of SFRSCC beam is also suggested. Comparisons are made between the suggested model and the fib Model Code 2010 model with experimental data. The results showed that the suggested model can estimate ultimate flexural capacity accurately.

Keywords: Self-consolidating concrete (SCC); Steel fibers; Ultimate flexural capacity; Crack pattern; Longitudinal reinforcement ratio; Prediction Model

1 Introduction

Plain concrete is a brittle material with a low tensile strength, cracking in concrete occurs at relatively low loads. Randomly distributed short, discrete steel fibers are usually added to improve the tensile properties of the composite, especially the post-cracking behaviour. Fibers have been found to control crack propagation, prevent large crack width, increase ultimate flexural strength, toughness and stiffness, and reduce deflection of concrete beams. One of the most important functions of steel fibers in concrete is the ability to transfer tension stresses across the cracked section, providing residual strength. The magnitude of residual strength depends on the fiber dispersion and interfacial action between fiber and concrete matrix [1-5]. The workability of fresh concrete was found to be damaged by the addition of steel fibers [6,7]. Furthermore improper compaction and placement may hinder the random dispersion of fibers within structural elements [8].

Self-consolidating concrete (SCC) is an innovation in concrete technology that is able to flow under its own weight, completely filling formwork and achieving full

compaction with no vibration effort. SCC can achieve good compaction without segregation, even in congested reinforcement members [9]. Combining benefits of SCC in the fresh state and those resulting from the addition of steel fibers in the hardened state, a high performance material, designated as steel fiber reinforced self-consolidating concrete (SFRSCC), is obtained. The main difference between SFRSCC and traditional SFRC is that the fiber content of SFRC is mainly determined by the post-cracking behaviour of the composite, while the fiber content of SFRSCC is mainly restricted by the workability of fresh SCC [10]. The use of SCC may help in guaranteeing a more uniform dispersion of fibers, thanks to both its rheological stability and self-placability [11]. Uniform distribution of fibers results in improved performances in the hardened state, especially the bond property between the steel fiber and the concrete matrix [12-14].

Plenty of researches, however, have so far been confined to mix design and material properties of SFRSCC [12-16]. The research regarding structural members of SFRSCC is still limited. Several researchers [10,17-18] investigated the shear behaviour of full-scale SFRSCC beams, and have indicated enhanced shear strength, reduced cracking width and deflection due to the addition of steel fibers. As a major area of fiber use in structural engineering, it is necessary to investigate the effects of fiber reinforcement on the flexural behaviour of reinforced self-consolidating concrete structural member. Barros et al. [8,19-20] believed that applying SFRSCC to thin slabs (supported on columns) or building façade panels were promising structural applications. Flexural and punching tests on panel prototypes were carried out and enhanced load carrying capacity was observed with the addition of fibers. But the fiber effect was reduced with the increasing of longitudinal reinforcement ratios, which agrees with the present study. Kassimi et al. [21] proposed the use of fiber reinforced SCC to repair damaged or deteriorated beams. Self-consolidating concrete and mortars reinforced with either steel or polypropylene fibers were used, proving their efficacy in restoring the load bearing capacity compared with that of the undamaged beams. In the structural applications above mentioned, SFRSCC was just used as a kind of special building material. In order to extend the use of SFRSCC by designers/engineers in practical applications, investigation on flexural behaviour of full-scale beam element casted by SFRSCC is necessary and a reasonable design model for estimating the ultimate flexural strength of SFRSCC beams is also needed.

The current study presents the results of the effect of steel fibers on the flexural behaviour of reinforced SCC beams. The major aim of this program is to evaluate the possibility of partially replacing the longitudinal reinforcements by macro steel fibers, and to study the effect of steel fiber on the ultimate flexural strength, steel reinforcement strain, midspan deflection and crack pattern of reinforced SCC beams. Interesting crack pattern that only one large crack developed in pure bending section of SFRSCC beam after yield of steel rebar was observed, which could also be found in literatures [22-24]. A prediction model is also developed for predicting the ultimate flexural capacity of the SFRSCC beams. The contribution of the fibers in the tension zone is considered, which takes into account the stress transfer mechanism between fiber and concrete matrix across the cracking section. The adequacy of the suggested

model is demonstrated by experimental data from the current study and published literatures and also compared with the fib Model Code 2010 [25].

2 Experimental program

In order to investigate the fiber contribution to the mechanical behaviour of conventional reinforced self-consolidating concrete beams, seven full-scale beams have been tested up to failure under a four-point loading scheme. The main variables considered in the study were the amount of longitudinal reinforcement as well as the fiber contents in the beams.

2.1 Materials

2.1.1 Mix proportion of concrete

The designed compressive strength of the self-consolidating concrete (SCC) was 60 MPa and the mix proportion is given in **Table 1**. P.O 52.5R Portland cement and fly ash were employed in this research. The coarse aggregates were crushed gravel and had specific mass of 2630 kg/m³, with particle size ranging from 5 to 10 mm. The fine aggregates were natural river sand and had fineness modulus of 2.6, with particle size of 0-5 mm. Polycarboxylate superplasticizer was also added to improve the workability.

Steel rebars of diameter 16 mm, 18 mm and 20 mm were used as longitudinal reinforcements. The detail properties of steel rebars are summarized in **Table 2**. The ratios of tensile reinforcements for the singly reinforced concrete beams are 0.76% (2 Φ 16), 0.96% (2 Φ 18) and 1.18% (2 Φ 20). The steel rebar used had a specific mass of 7850 kg/m³ with an elastic modulus of 200 GPa and Poisson's ratio of 0.3.

Hooked-ended macro steel fiber (see **Fig. 1**) (fiber length $l_f = 60$ mm, equivalent diameter $d_f = 0.75$ mm, aspect ratio $l_f/d_f = 80$, approximately 5,000 pieces/kg, tensile strength 1100 N/mm²) was added with two different contents (30 or 50 kg/m³, corresponding to a volume fraction V_f of 0.38% and 0.64%, respectively).

2.1.2 Specimen preparation

All beams having the same dimension of b (width) \times h (depth) \times l (length) = 200 mm \times 300 mm \times 2400 mm, were simply supported with 2100 mm span. **Fig. 2** shows the beam geometry and the reinforcement details. The size and the main variables of the seven full-scale beams are listed in **Table 3**. In Table 3, each beam is designed by the steel fiber content and reinforcement amount. The first two letters BS denote a simply supported beam; the third letter A (B or C) corresponds to different reinforcement ratios ranging from 0.76% to 1.18%; the last two letters SF (or PC) represent beam with steel fibers (or plain concrete without fibers); the digit 30 (or 50) indicates the steel fiber content in terms of kg/m³. For instance, BS-A-SF30 refers to a beam with 30 kg/m³ steel fibers and reinforcement ratio of 0.76%. To prevent the premature shear failure, two leg stirrups having a diameter of 6.5 mm were placed at 80 mm spacing in the zone outward the two point loads, where shear action is present.

The workability of fresh SFRSCC was evaluated according to EFNARC [16]. The test methods used in this research included slump flow test and L-box test. The consistency and filling ability of concrete was evaluated using the slump flow test.

With the L-box test, it is possible to measure different properties such as flowability, passing ability, and segregation resistance. Standard cubic specimens ($150 \times 150 \times 150$ mm) were cast for measurement of concrete compressive strength. After 24 hours, the concrete cubes were demoulded, marked and transferred to the curing room at a temperature of 20 ± 2 °C and humidity of about 95% until testing at 28 days.

2.1.3 Test procedure

The beams were tested under a displacement-controlled procedure by means of a hydraulic servo testing machine having a maximum load capacity of 10,000 kN and a steel distributive girder on the top face of the beam (see **Fig. 3**). The load was applied step by step to the beam at a rate of 20 kN per step with a displacement rate of 0.3 mm/min by the testing machine. After yielding of steel reinforcement, the loading rate was progressively increasing up to 0.6 mm/min, and this rate was maintained up to failure. The vertical deflections at the midspan and under the two loading points were measured by three linear variable displacement transducers (LVDTs) with maximum measurement range of 50 mm. Electrical-resistance strain gauges were also used to record the strains in the longitudinal rebar at several selected locations, as shown in **Fig. 3**. All measurements were automatically read and stored in the data-acquisition system. The data logger was connected to the digital controller of the testing machine. At the end of each loading step, cracks were sketched with two markers of different colours to record the crack propagation across the depth of the beam.

3 Experimental results and discussion

3.1 Workability and compressive strength

The experimental results of workability of fresh SFRSCC are presented in **Table 4**. The factor d_m represents the average final slump flow diameter, while factor T_{500} represents the time taken for the mixture to reach the 500 mm spread circle in slump flow test. Parameters T_{200} and T_{400} represent the time taken for the mixture to reach 200 mm and 400 mm in the L-box. The ratio H_2/H_1 represents the passing ability in the L-box. It can be seen from **Table 4** that all parameters regarding workability meet the requirements of SCC according to EFNARC [26].

The 28-days cubic compressive strength $f_{cu,28}$ and equivalent cylinder compressive strength $f'_c,28$ of steel fiber reinforced SCC are listed in **Table 4**. The addition of fibers aids in converting the brittle properties of concrete to a ductile material, however no significant trend of improving compressive strength was observed.

3.2 Flexural tensile strength and toughness

The flexural tensile behaviour of SFRSCC is determined by performing three point bending tests on $150 \times 150 \times 550$ mm notched beams (on a 500 mm span), according to the RILEM TC162-TDF [27]. The depth of the notch is 25 mm. Fig. 4 shows the load-CMOD curves of concrete beams with different dosages of steel fibers. Note that the addition of 50 kg/m^3 steel fibers determines a deflection-hardening behaviour under flexure. The residual flexural tensile strength parameters (f_{R1} , f_{R3}), proposed by RILEM TC 162-TDF [27], to characterize and simulate the post-cracking

tensile behaviour of SFRSCC have been calculated. For the two FRC materials tested, f_{R1} resulted in 6.36 MPa and 11.56 MPa, while f_{R3} was 4.68 MPa and 10.03 MPa, respectively with the addition of 30 and 50 kg/m³ steel fibers. It can be seen that fibers demonstrate strong influence on the post-cracking tensile behaviour with the increasing of fiber dosages.

3.3 Load-midspan deflection behaviour

Fig. 5 shows the load–midspan deflection curves for the SFRSCC beams with different longitudinal reinforcement ratios. **Table 5** summarizes the failure modes and test results at different loading stages. The addition of steel fibers may enhance the cracking load, yielding load and ultimate load of SCC beams.

From **Fig. 5a** and **Table 5**, it can be seen that, the cracking load that was not significantly affected by the addition of steel fibers. However, after cracking of the beam, great difference is observed due to enhanced flexural stiffness of the beam with the addition of steel fibers. Steel fibers bridge the crack and undertake part of the load released by the cracked concrete. The yielding load and ultimate load were remarkably enhanced, while the midspan deflections corresponding to yielding point and ultimate point greatly decreased with the increase of steel fiber contents. Compared to reference beam BS-A-PC, the yielding load P_y increased by 19.0% and 34.5% respectively, while the ultimate load P_u was enhanced by 11.4% and 18.8% respectively due to the inclusion of 30 kg/m³ and 50 kg/m³ steel fibers. For higher longitudinal reinforcement ratio (**Fig. 5b**), similar trend of fiber effect on the flexural capacity of reinforced SCC beam can be observed, but the reinforcing effect of steel fiber reduces. Compared to reference beam BS-B-PC, it is noted that inclusion of 30 kg/m³ and 50 kg/m³ steel fibers enhances the yielding load P_y by 16.3% and 24.5% respectively, and increases the ultimate load P_u by 5.3% and 9.6% respectively.

The combination use of steel fibers and traditional steel rebars in concrete structures is a good option [28]. On the one hand, the reinforcing bars undertake the main bearing capacity of the structural member in bending. On the other hand, the steel fibers cross the crack and give the cracking matrix a reliable post-cracking tensile strength and ductility. Compared to reference beam BS-B-PC ($\rho_s = 0.96\%$), the yielding load and ultimate load of the SFRSCC beam BS-A-SF50 ($\rho_s = 0.76\%$) were enhanced by 6.1% and 1.5%, respectively (**Fig. 5a**). It illustrates that adding 50 kg/m³ steel fiber can reduce the longitudinal reinforcement ratio (ρ_s) by about 0.2%. However, compared to reference beam BS-C-PC ($\rho_s = 1.18\%$), adding 50 kg/m³ in lower reinforcement ratio beam BS-B-SF50 ($\rho_s = 0.96\%$) does not sufficiently contribute to yielding and ultimate flexural capacity (**Fig. 5b**).

3.4 Steel reinforcement strain behaviour

The steel reinforcement strains were automatically measured continuously through the whole testing procedures. **Fig. 6** depicts the load-steel strain curves for the SFRSCC beams at different load level. It indicates that there is no significant effect on the steel reinforcement strain before cracking of the SFRSCC beam with the addition of steel fiber. As for series-A (reinforcement ratio of 0.76%) beams, at load level 40 kN, the steel reinforcement strains in beams BS-A-SF30 and BS-A-SF50 were almost the same as that of beam BS-A-PC. As far as series-B (reinforcement

ratio of 0.96%) beams considered, the same trend was observed. However, after cracking of the SFRSCC beam, the strain in longitudinal reinforcement is greatly reduced due to the presence of steel fiber compared with the reference beam. As for series-A (reinforcement ratio of 0.76%) beams, compared with beam BS-A-PC at load level 100 kN, the steel reinforcement strains in beams BS-A-SF30 and BS-A-SF50 decreased by 50% and 55%, respectively. The same trend was also observed for series-B (reinforcement ratio of 0.96%) beams. Before cracking, the concrete, steel reinforcement and steel fiber show strain compatibility, and during this stage the contribution of steel fiber for tensile strength of concrete is limited. After cracking, however, the strain compatibility is disturbed and steel fibers cross the cracks to transfer the load together with the conventional longitudinal reinforcement. Thus, the strain in steel rebars decreased due to the addition of steel fibers at a given load level after cracking of the beam.

3.5 Cracking behaviour

In addition to the load-midspan deflection and load-steel reinforcement strain behaviour of SFRSCC beams, the cracking characteristics have been also observed during the tests. **Fig. 7** shows the crack pattern of the full-scale SFRSCC beams at the end of the test. The presence of steel fibers in the concrete was seen to increase the number of cracks and reduce the crack width and crack spacing.

At the beginning of the tests, under relatively low loading levels, there were several tiny flexural cracks that started to develop in the constant moment region between the two loading points. As can be seen in **Fig. 7**, well distributed flexural cracks continued to develop with the increasing of external load in the beams without fibers (beams BS-A-PC or BS-B-PC). As for beams with fibers (beams BS-A-SF50 or BS-B-SF50), different crack pattern was observed during the increase of external load. Only one large crack in the constant moment region developed (see **Fig. 7**) after yield of steel rebar. Similar crack patterns could also be found in the literatures [22-24]. Compared to beams without steel fibers, reduced deflection can be obtained at the same load level with the addition of steel fibers. This may due to the increased bond between steel rebar and concrete matrix caused by the confining action of the steel fiber [29-31]. It is noted that, for beams of higher reinforcement ratio, the confining effect of the fibers is expected to be reduced, thus reducing the localization effect, as observed in the beam BS-B-SF50 (see **Fig. 7**).

4 Flexural analysis of SFRSCC beams

In traditional flexural theory [32], the tensile strength of concrete after cracking is generally neglected in estimating the ultimate flexural capacity of reinforced concrete beams. This is because the tensile strength of concrete is much less than the compressive strength. However, in steel fiber reinforced concrete, the main benefits of the fibers are effective after matrix cracking has occurred, since fibers crossing the crack guarantee a certain level of stress transfer between both faces of the crack, providing residual strength. The magnitude of this residual strength depends on the fiber, matrix, and fiber-matrix properties [17]. The established theory of geometrical

probability (integral geometry, stereology) offers a straightforward approach to spatial modeling of fibers reinforcing a leading crack in concrete. These theoretical principles are introduced, discussed, and applied to SFRC in tension by Stroeven and Hu [33,34], yielding general expressions for fiber contribution to stress transfer over the leading crack for the cracked beam. Therefore, contribution of fibers can be taken into account in the flexural analysis of beams.

The ultimate flexural strength analysis presented in this paper is based on the conventional compatibility and equilibrium conditions used for normal reinforced concrete, apart from that the contribution of the steel fibers in the tension zone are taken into account.

4.1 Stress-strain relationship of materials

A Hognestad stress-strain relationship [35] was used for concrete in compression

$$\sigma_c = \begin{cases} f'_c \left[1 - \left(1 - \frac{\varepsilon_c}{\varepsilon_0} \right)^2 \right] & 0 < \varepsilon_c \leq \varepsilon_0 \\ f'_c \left(1 - 0.15 \frac{\varepsilon_c - \varepsilon_0}{\varepsilon_{cu} - \varepsilon_0} \right) & \varepsilon_0 < \varepsilon_c \leq \varepsilon_{cu} \end{cases} \quad (1)$$

where f'_c is the compressive strength of concrete; ε_0 is the strain at peak stress of concrete, taken as 0.002; and ε_{cu} is the ultimate strain of concrete, taken as 0.003 for plain concrete and 0.0035 for steel fiber reinforced concrete [1].

The stress-strain relation of longitudinal reinforcement used in the study is expressed as:

$$\sigma_s = \begin{cases} E_s \varepsilon_s & 0 < \varepsilon_s \leq \varepsilon_y \\ f_y + \frac{f_{tu} - f_y}{\varepsilon_{tu} - \varepsilon_y} \varepsilon_s & \varepsilon_y < \varepsilon_s \leq \varepsilon_{tu} \end{cases} \quad (2)$$

where E_s is the elastic modulus of reinforcement; f_y , f_{tu} are the yielding and ultimate strength of reinforcement in tension, respectively; ε_y is the yielding strain of reinforcement and is calculated as $\varepsilon_y = f_y/E_s$; and ε_{tu} is ultimate tensile strain of reinforcement, taken as 2.5% according to RILEM [36].

Regarding the tensile behaviour of steel fiber reinforced concrete, the composite materials concept may be introduced to describe post-cracking tensile strength of SFRC. The flexural tensile strength of SFRC may be described as the sum of matrix strength and fiber strength as follows:

$$\sigma_{ct} = \sigma_m (1 - V_f) + \sigma_{fu} V_f \quad (3)$$

in which σ_{ct} stands for tensile strength of SFRC; σ_m is the tensile strength of concrete matrix; σ_{fu} is the stress transfer capability of steel fiber perpendicular to crack; V_f is the volume fraction of steel fiber.

This paper does not aim to discuss this law of mixtures. It merely focuses on the term σ_{fu} . Regarding σ_{fu} , there are several models available considering the contribution of fibers for evaluating the ultimate flexural capacity of beams in the published literatures [37-39]. However, most of these models are semi-empirical, and

the mechanism of stress transfer of steel fiber is not dealt with. Failure of the RC or SFRC elements may be governed not by average stresses, but by local stresses that occur at a crack. Load component transferred perpendicular to crack is due to pullout friction resistance and shearing over crack at the intersection of steel fiber and leading crack (see **Fig. 8**). The critical crack direction is assumed normal to the principal tensile strain direction. For a fiber with an angle θ_i with the loading direction, the load component perpendicular to the crack is expressed as follows [33,34]:

$$P_{i\perp}(\theta) = \pi d_f \tau_f e_i [\cos \theta_i + f \sin \theta_i] \quad (4)$$

where e_i is the effective embedment length of fibers, $e_i \leq l_f/2$; d_f is the diameter of fibers; f is the friction resistance of a fiber sheared over the crack edge. **Eq. (4)** has to be averaged over all active fibers, yielding for an isotropic uniform random (IUR) bulk fiber system [34]:

$$\bar{P}_{\perp} = \frac{1}{6} \pi d_f l_f \tau_f (1 + f) \quad (5)$$

where l_f is the length of steel fibers.

Multiplying the load of a single fiber by the number of fibers intersecting the crack, the stress transferred over the crack in the loading direction is obtained

$$\sigma_{fu} = \bar{P}_{\perp} N_A \quad (6)$$

where N_A is the number of fibers N per unit area A , $N_A = \frac{2}{\pi} \frac{V_f}{d^2}$ (for 3D) [34].

Considering Eq. (5) and Eq. (6), the stress transfer capability perpendicular to crack can be written as:

$$\sigma_{fu} = \frac{1}{3} \alpha \tau_f V_f (1 + f) \quad (7)$$

where α is the aspect ratio ($\alpha = l_f/d_f$, l_f and d_f are the length and diameter of fibers, respectively); τ_f is the average fiber matrix interfacial bond stress; V_f the volume fraction of fibers; f is the coefficient of friction between concrete and fiber sheared over the crack edge, taken as 1/3 recommended by Stroeven [34].

4.2 Flexural analysis of SFRSCC beams

The stress and strain distributions at failure are shown in **Fig. 9**. The height of the elastic uncracked zone of concrete is very small compared to the neutral axis depth x . Therefore it is assumed that the tensile contribution of the steel fibers is represented by a rectangular stress block over the whole tension zone of the beam (see **Fig. 9c**).

Dividing the cross section of concrete along the height into m strips, based on the plane section assumption, the stresses of concrete and steel reinforcement at a given depth c to the neutral axis of the section in beams can be determined by Eqs. (1) and (2) according to the following equations:

$$\varepsilon_k = \phi_i \left(c - k \Delta h + \frac{\Delta h}{2} \right) \quad (8)$$

$$\varepsilon_s = \phi_1 (d - c) \quad (9)$$

$$\varepsilon_{ct} = \phi_1 (h - c) \quad (10)$$

where ε_k is the compressive strain of the k -th strip in concrete; ϕ_i is the equivalent curvature; and ε_{ct} is the tensile strain of concrete in tension.

The equilibrium condition of force and moment for the selected beam section results in:

$$P = \sum_{k=1}^m \sigma_k(\varepsilon) b \Delta h - f_s A_s - \sigma_{fu} b (h - c) \quad (11)$$

$$M = \sum_{k=1}^m \sigma_k(\varepsilon) b \Delta h \left(\frac{h}{2} - k \Delta h + \frac{\Delta h}{2} \right) + f_s A_s \times (d - c) + \sigma_{fu} b (h - c) \left(\frac{h - c}{2} \right) \quad (12)$$

where m is the total number of concrete strip; Δh is the width of each strip and $\Delta h = h/m$; h and b are the depth and width of the cross section, respectively; d is the effective depth of the cross section; σ_k is the compressive stress in the k -th concrete strip; f_s is the stress of reinforcement in tension; and A_s is the area of reinforcement in tension. The flow chart for the analysis of the suggested model is shown in **Fig. 10**.

For comparison, a simple flexural analysis on the basis of the fib Model Code 2010 [25] is applied to compare with the suggested model. Apart from the assumptions of compressive stress blocks for the concrete stresses and the ideal elastic plastic behaviour for steel reinforcement, two simplified stress-crack opening laws shown in **Fig. 11** are used to characterize the post-cracking behaviour of SFRC in uniaxial tension, where f_{Fts} represents the serviceability residual strength, defined as the post-cracking strength for serviceability crack openings, and f_{Ftu} represents the ultimate residual strength. For simplicity, the rigid-plastic model is adopted in the present study and parameter f_{Ftu} is determined according to the approach described in section 3.2 using the following expression:

$$f_{Ftu} = \frac{f_{R3}}{3} \quad (13)$$

Based on the equilibrium condition of force and moment, the ultimate moment M_u can be calculated by:

$$M_u = A_s f_y \left(d - \frac{x}{2} \right) + f_{Ftu} b (h - c) \left(\frac{h}{2} + \frac{c}{2} - \frac{x}{2} \right) \quad (14)$$

where, x is the depth of rectangular stress blocks.

4.3 Comparisons with test results

Table 6 shows the comparison of predicted-to-experimental ultimate flexural capacity data for the suggested model (12) and Model Code 2010 (MC2010) formula (14). From **Table 6**, it can be seen that the solutions based on the suggested method agree well with the experimental results of fiber reinforced SCC beams, having a mean of 0.922 and a COV (coefficient of variation) of 0.071. However, the MC2010 method provides a conservative prediction for the ultimate flexural capacity of fiber reinforced SCC beams, having a mean of 0.831 and a COV of 0.091. It illustrates that

the suggested model can provide better fit with the experimental results.

To extend the validity of the suggested method for the ultimate flexural capacity of SFRC beams, the prediction was also made for beams that had been tested in previous studies [23,40-41]. The dimensions and properties are summarized in **Table 7**. Compared measured and predicted ultimate flexural capacity in **Table 7**, it can be seen that the prediction model considering the stress transfer mechanism between fiber and concrete matrix across the cracking section agree well with the experimental results of the reinforced SFRC beams, having a mean value of 1.057 and a COV of 0.129. It may be said that the fiber reinforced concrete theory taking into account the distribution and orientation of fibers across the cracked plane can not only be used to predict the flexural behaviour of reinforced SFRC beams, but also can be extended to reinforced self-consolidating concrete beams containing steel fibers.

5 Conclusions

An experimental program was performed and a total of seven full-scale steel fiber reinforced self-consolidating concrete (SFRSCC) beams were tested. The load-midspan deflection relationship and load–steel reinforcement strain curves were automatically measured and stored using a data-acquisition system. In addition, the cracking characteristics, including crack width, crack spacing, and crack pattern have also been investigated. Finally, a method incorporating fiber effects in the flexural analysis of singly reinforced concrete beams is suggested and compared with experimental data from the current study and published literatures and also compared with MC2010 model.

From the present experiment and analytical study on the flexural behaviour of SFRSCC beams, the following conclusions may be drawn:

- The ultimate flexural capacity of SFRSCC beams is increased significantly with increasing of fiber contents, and the effect of steel fibers is more pronounced for beams with relatively lower reinforcement ratio.
- Before cracking of SFRSCC beam, the influence of steel fibers on the steel reinforcement strain is small. However, after cracking, steel fibers play an important role in reducing the steel reinforcement strain compared with the beams without steel fibers at the same load level.
- With the incorporation of steel fiber, the number of cracks increased while crack width and spacing decreased. A single major crack developing in fiber reinforced beams termed as deformation localization effect was observed. This phenomenon decreases with increasing of longitudinal reinforcement ratio.
- Adding 50 kg/m³ steel fiber in beam with reinforcement ratio 0.76% can perform better than beam with reinforcement ratio 0.96% in terms of yielding and ultimate load. It illustrates that adding 50 kg/m³ steel fiber in reinforced SCC beam can replace reinforcement ratio about by 0.2%. However, the same amount of steel fiber in beam with 0.96% reinforcement ratio can't achieve yielding and ultimate load similar to the beam with 1.18% reinforcement ratio.
- A model for predicting the ultimate flexural capacity of SFRSCC beams is suggested. The model considers the fiber contribution to concrete in tension zone by taking into account the stress transfer mechanism between fiber and concrete

matrix across the cracking section. The results from predicted model are found to agree well with test data obtained by authors and other researchers. Comparison of the suggested model and MC2010 model also illustrates that the former one can provide better fit with the experimental results. It demonstrates that the suggested model can be used to predict the ultimate flexural capacity of fiber reinforced SCC beams accurately.

Nomenclature:

BS-A-SF30 = steel fiber reinforced self-consolidating concrete beams with fiber content of 30 kg/m^3 and a longitudinal reinforcement ratio of 0.76%

CMOD = crack mouth opening displacement

d_m = the average of final diameter in slump flow test

T_{500} = the time for concrete to reach the 500 mm spread circle in the slump test

T_{200}, T_{400} = time taken for the mixture to reach 200 mm and 400 mm in the L-box test

H_2/H_1 = the blocking ration in the L-box test

f_{R1} = residual flexural tensile strength corresponding to CMOD at 0.5 mm

f_{R3} = residual flexural tensile strength corresponding to CMOD at 2.5 mm

f_{Fts} = serviceability residual strength

f_{Ftu} = ultimate residual strength

P_{cr} = flexural cracking load

δ_{cr} = midspan deflection corresponding to cracking load

P_y = the yielding load

δ_y = midspan deflection corresponding to yielding load

P_u = the ultimate load

δ_u = midspan deflection corresponding to ultimate load

σ_c = compressive stress of concrete

ϵ_c = compressive strain of concrete

ϵ_0 = compressive strain corresponding to peak compressive stress

ϵ_{cu} = ultimate compressive strain of concrete

σ_s = steel reinforcement stress

f_y = yielding strength of longitudinal reinforcement

f_{tu} = tensile strength of longitudinal reinforcement

ϵ_s = strain in steel reinforcement

ϵ_y = yielding strain corresponding to yielding strength of steel reinforcement

ϵ_{tu} = ultimate strain of steel reinforcement

σ_{ct} = tensile strength of the composites

σ_{fu} = post-cracking tensile strength of the composites

V_f = volume fraction of fiber

α = the aspect ratio of fiber

l_f = fiber length

d_f = fiber diameter

N_A = fiber number per unit area

f = coefficient of friction between concrete and fiber sheared over the crack edge

A_s = steel reinforcement area

b = width of the beam cross section

d = effective depth of the beam cross section
 h = depth of the beam cross section
 c = depth of neutral axis
 x = depth of rectangular compressive stress blocks
 ρ_s = longitudinal reinforcement ratio, $A_s/(bd)$
 a/d = shear span-to-depth ratio

Acknowledgements

The first three authors gratefully acknowledge the National Natural Science Foundation of China: Grant: 51078058 and Grant: 51121005. The last author was partially supported by CMAT with the Portuguese Funds from the “Fundação para a Ciência e a Tecnologia”, through the Project PEstOE/MAT/UI0013/2014.

References

- [1] ACI Committee 544. Design considerations for steel fiber reinforced concrete. American Concrete Institute, Farmington Hills, MI, 1999.
- [2] Olivito RS, Zuccarello FA. An experimental study on the tensile strength of steel fiber reinforced concrete. *Compos Part B: Eng* 2010; 41(3):246-255.
- [3] Soutsos MN, Le TT, Lampropoulos AP. Flexural performance of fibre reinforced concrete made with steel and synthetic fibres. *Constr Build Mater* 2012; 36(0):704-710.
- [4] Caggiano A, Cremona M, Faella C, Lima C, Martinelli E. Fracture behavior of concrete beams reinforced with mixed long/short steel fibers. *Constr Build Mater* 2012; 37(0):832-840.
- [5] Chi Y, Xu L, Zhang Y. Experimental study on hybrid fiber-reinforced concrete subjected to uniaxial compression. *J Mater Civ Eng* 2014; 26(2):211-218.
- [6] Bayasi MZ, Soroushian P. Effect of steel fiber reinforcement on fresh mix properties of concrete. *ACI Mater J* 1992; 89(4):369-374.
- [7] Ding Y, Liu S, Zhang Y, Thomas A. The investigation on the workability of fibre cocktail reinforced self-compacting high performance concrete. *Constr Build Mater* 2008; 22(7):1462-1470.
- [8] Barros JAO. Technology, design and applications of steel fibre reinforced self-compacting concrete. 6th International Conference Fibre Concrete 2011-Technology, Design, Application, 2011.
- [9] Cattaneo S, Giussani F, Mola F. Flexural behaviour of reinforced, prestressed and composite self-consolidating concrete beams. *Constr Build Mater* 2012; 36(0):826-837.
- [10] Ding Y, You Z, Jalali S. The composite effect of steel fibres and stirrups on the shear behaviour of beams using self-consolidating concrete. *Eng Struct* 2011; 33(1):107-117.
- [11] Ferrara L, Park Y-D, Shah SP. Correlation among fresh state behavior, fiber dispersion, and toughness properties of sfrcs. *J Mater Civil Eng* 2008; 20(7):493-501.
- [12] Pająk M, Ponikiewski T. Flexural behavior of self-compacting concrete

- reinforced with different types of steel fibers. *Constr Build Mater* 2013; 47(0):397-408.
- [13] Goel S, Singh S, Singh P. Flexural fatigue strength and failure probability of self-compacting fibre reinforced concrete beams. *Eng Struct* 2012; 40(0):131-140.
- [14] Khaloo A, Molaei Raisi E, Hosseini P, Tahsiri H. Mechanical performance of self-compacting concrete reinforced with steel fibers. *Constr Build Mater* 2014; 51(0):179-186.
- [15] Ferrara L, Park Y-D, Shah SP. A method for mix-design of fiber-reinforced self-compacting concrete. *Cem Con Res* 2007; 37(6):957-971.
- [16] Ponikiewski T, Katzer J. Properties of fresh SCC mix reinforced by different types of steel and polymer fibre. *Constr Build Mater* 2014; 62(0):96-101.
- [17] Ding Y, Zhang F, Torgal F, Zhang Y. Shear behaviour of steel fibre reinforced self-consolidating concrete beams based on the modified compression field theory. *Compos Struct* 2012; 94(8):2440-2449.
- [18] Greenough T, Nehdi M. Shear behavior of fiber-reinforced self-consolidating concrete slender beams. *ACI Mater J* 2008, 105(5):468-477.
- [19] Barros JAO, Pereira EN, Santos S. Lightweight panels of steel fiber-reinforced self-compacting concrete. *J Mater Civil Eng*, 2007, 19(4): 295-304.
- [20] Pereira EN, Barros JAO, Camões A. Steel fiber-reinforced self-compacting concrete: experimental research and numerical simulation. *J Struct Eng* 2008; 134(8):1310-1321.
- [21] Kassimi F, El-Sayed AK, Khayat KH. Performance of Fiber-Reinforced Self-Consolidating Concrete for Repair of Reinforced Concrete Beams. *ACI Struct J* 2014; 111(6):1277-1286.
- [22] Schumacher P. Rotation capacity of self-compacting steel fiber reinforced concrete. Ph.D. thesis, Delft University of Technology, 2006.
- [23] Dancygier AN, Savir Z. Flexural behavior of HSFRC with low reinforcement ratios. *Eng Struct* 2006; 28(11):1503-1512.
- [24] Deluce JR, Vecchio FJ. Cracking behavior of steel fiber-reinforced concrete members containing conventional reinforcement. *ACI Struct J* 2013; 110(3):481-490.
- [25] Fib Model Code 2010. *fédération internationale du béton/International Federation for Structural Concrete*, Germany, 2013.
- [26] EFNARC. *Specification and guidelines for self-compacting concrete*. 2002.
- [27] RILEM TC 162-TDF. Test and design methods for steel fibre reinforced concrete: bending test (final recommendation). *Mater Struct* 2002; 35(11):579-582.
- [28] Yang Y, Walraven JC, den Uijl JA. Combined effect of fibers and steel rebars in high performance concrete. *Heron* 54 (2/3), 2009.
- [29] Chao SH, Naaman AE, Parra-Montesinos GJ. Bond behavior of strand embedded in fibre reinforced cementitious composites. *PCI J* 2006; 6:2-17.
- [30] Harajli M, Hamad B, Karam K. Bond-slip Response of Rebars Embedded in Plain and Fibre Concrete. *J Mater Civ Eng* 2002; 14(6):503-511.
- [31] Ding Y, Ning X, Zhang Y, Pacheco-Torgal F, Aguiar JB. Fibres for enhancing of the bond capacity between GFRP rebar and concrete. *Constr Build Mater* 2014;

51(0):303-312.

- [32] Park R, Paulay T. Reinforced concrete structures. New York: John Wiley & Sons, 1975.
- [33] Stroeven P, Hu J. Effectiveness near boundaries of fibre reinforcement in concrete. *Mater Struct* 2006; 39(10):1001-1013.
- [34] Stroeven P. Stereological principles of spatial modeling applied to steel fiber-reinforced concrete in tension. *ACI Mater J* 2009; 106(3): 213-222.
- [35] Hognestad E. A Study on Combined Bending and Axial Load in Reinforced Concrete Members. University of Illinois Engineering Experiment Station, University of Illinois at Urbana-Champaign, Urbana, IL, 1951:43-46.
- [36] RILEM TC 162-TDF. Test and design methods for steel fiber reinforced concrete: σ - ϵ design method: final recommendation. *Mater Struct* 2003; 36(10):560-567.
- [37] Swamy R, Al-Ta'an SaA. Deformation and ultimate strength in flexure of reinforced concrete beams made with steel fiber concrete. *ACI J* 1981; 78(5):395-405.
- [38] Lim TY, Paramasivam P, Lee SL. Analytical model for tensile behavior of steel-fiber concrete. *ACI Mater J* 1987; 84(4):286-298.
- [39] Lim TY, Paramasivam P, Lee SL. Behavior of reinforced steel-fiber-concrete beams in flexure. *J Struct Eng* 1987; 113(12):2439-2458.
- [40] Meda A, Minelli F, Plizzari GA. Flexural behaviour of RC beams in fibre reinforced concrete. *Compos Part B: Eng* 2012; 43(8):2930-2937.
- [41] Oh BH. Flexural analysis of reinforced concrete beams containing steel fibers. *J Struct Eng* 1992; 118(10):2821-2836.

Table list

Table 1 Mix proportion of SCC (kg/m³)

Cement	Fly ash	Water	Fine aggregate	Coarse aggregate	SP. ^a	W/B ^b
400	160	180	832	765	6.16	0.32

Note: ^a = Superplasticizer; ^b = Water to binder ratio (Binder = Cement + Fly ash).

Table 2 Physical and mechanical properties of steel rebars

Steel rebar	Diameter (mm)	Yield strength (MPa)	Tensile strength (MPa)	Hardening ratio	Percent elongation (%)
Φ 16	16	471	654	1.39	12.5
Φ 18	18	454	650	1.43	13.5
Φ 20	20	443	612	1.38	12.0

Table 3 Beam characteristics

Beams	$l \times b \times h$ (mm)	a/d	A_s (mm ²)	ρ_s (%)	Fibers
BS-A-PC	2400×200×300	3.0	402 (2 Φ 16)	0.76	--
BS-A-SF30		3.0	402 (2 Φ 16)	0.76	30 kg/m ³ ($V_f = 0.38\%$)
BS-A-SF50		3.0	402 (2 Φ 16)	0.76	50 kg/m ³ ($V_f = 0.64\%$)
BS-B-PC		3.0	509 (2 Φ 18)	0.96	--
BS-B-SF30		3.0	509 (2 Φ 18)	0.96	30 kg/m ³ ($V_f = 0.38\%$)
BS-B-SF50		3.0	509 (2 Φ 18)	0.96	50 kg/m ³ ($V_f = 0.64\%$)
BS-C-PC		3.0	628 (2 Φ 20)	1.18	--

Table 4 Fresh and mechanical properties of SFRSCC mixture

Fiber contents (kg/m ³)	Slump flow		L-box			$f_{cu,28}$ (MPa)	$f'_c,28$ (MPa)
	d_m (mm)	T_{500} (s)	H_2/H_1	T_{200} (s)	T_{400} (s)		
0	780	3.1	0.91	2.2	5.1	65.3	52.2
30	740	3.4	0.87	2.7	6.4	67.0	53.6
50	700	4.4	0.81	4.9	9.7	66.8	53.4

Table 5 Failure mode and test results at different loading stages

Specimen Notation	f_{cu} (Mpa)	f'_c (MPa)	At cracking		At yielding		At ultimate		Failure mode
			P_{cr} (kN)	δ_{cr} (mm)	P_y (kN)	δ_y (mm)	P_u (kN)	δ_u (mm)	
BS-A-PC	65.3	52.2	34	0.45	116	5.3	167	43.4	Flexural
BS-A-SF30	67.0	53.6	35	0.53	138	4.9	186	40.4	Flexural
BS-A-SF50	66.8	53.4	37	0.58	156	5.2	198	30.7	Flexural
BS-B-PC	75.6	60.5	39	0.58	147	5.8	195	42.4	Flexural
BS-B-SF30	77.4	61.9	41	0.51	171	4.9	206	38.5	Flexural
BS-B-SF50	68.4	54.7	37	0.41	183	5.5	215	33.7	Flexural
BS-C-PC	63.3	50.6	39	0.57	186	6.2	227	37.7	Flexural

Table 6 Comparison of predicted ultimate moment with measured ultimate moment

Beams	Measured moment, $M_{u,exp}$ (kN.m)	Predicted moment, $M_{u,pre}$ (kN.m)		Ratio = $M_{u,pre} / M_{u,exp}$	
		Suggested formula	Model Code 2010	Suggested formula	Model Code 2010
BS-A-PC	66.9	55.6	48.5	0.831	0.725
BS-A-SF30	74.5	70.8	60.6	0.950	0.814
BS-A-SF50	79.5	72.7	73.6	0.914	0.925
BS-B-PC	78.2	67.9	59.0	0.868	0.755
BS-B-SF30	82.4	83.4	71.1	1.012	0.863
BS-B-SF50	86.1	85.1	83.2	0.988	0.967
BS-C-PC	90.8	80.9	69.9	0.891	0.770
Mean				0.922	0.831
COV				0.071	0.091

Figures

Fig. 1 Macro steel fibers.

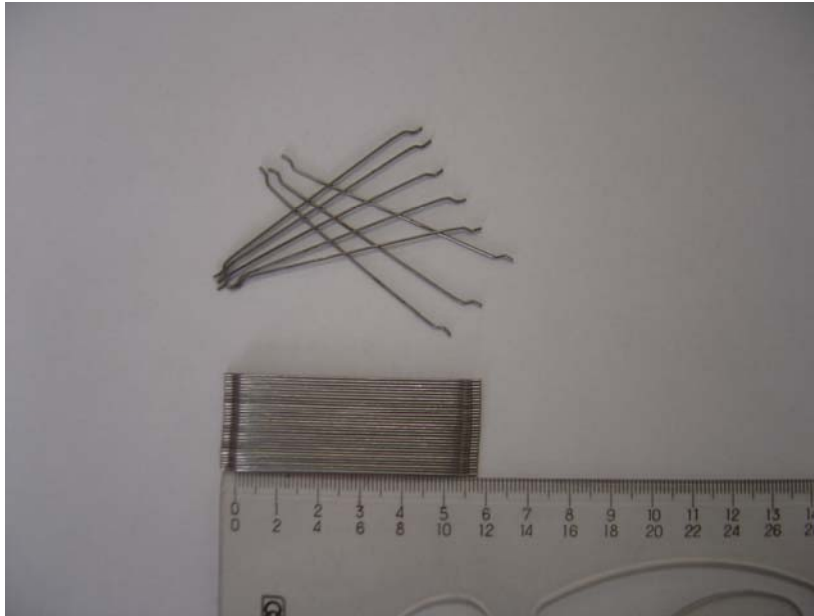


Fig. 2 Geometry of the tested beam (units: mm).

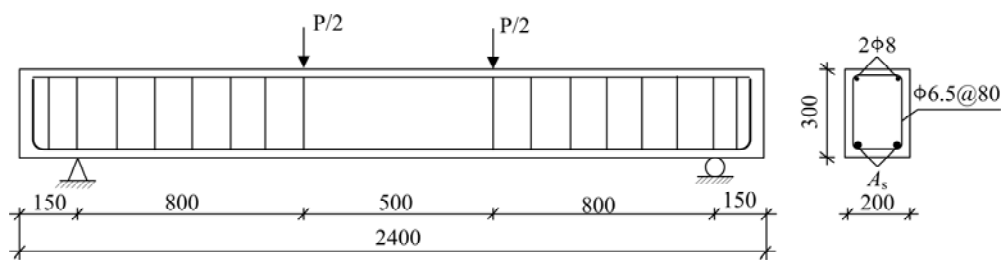


Fig. 3 Loading and measuring arrangement of test beams (units: mm).

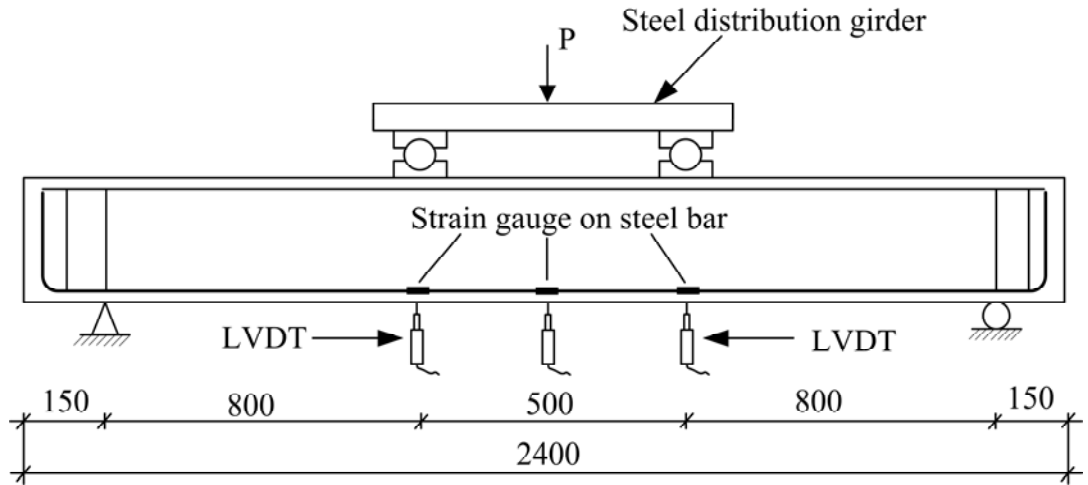


Fig. 4 Load-CMOD curves of SFRSCC beams under flexure

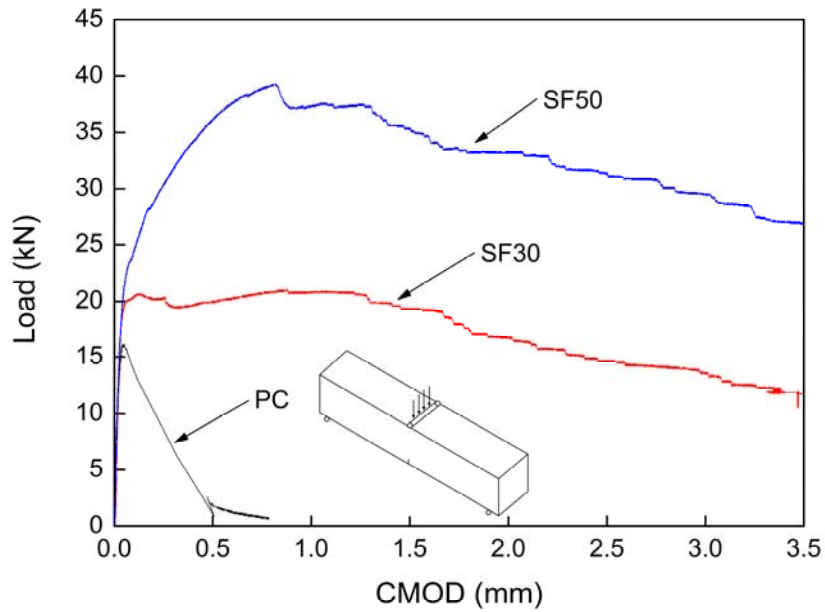


Fig. 5 Load-midspan deflection curves with different longitudinal reinforcement ratios: (a) BS-A; (b) BS-B.

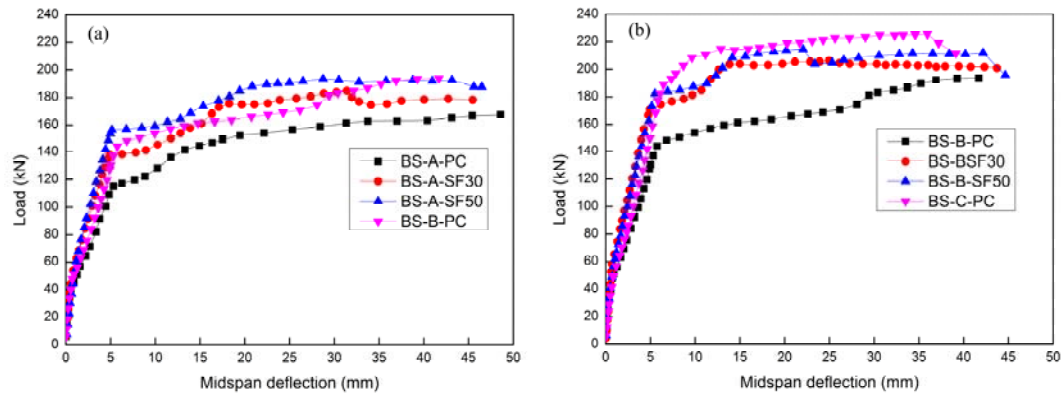


Fig. 6 Load-longitudinal reinforcement strain curves with different steel fiber contents: (a) BS-A; (b) BS-B.

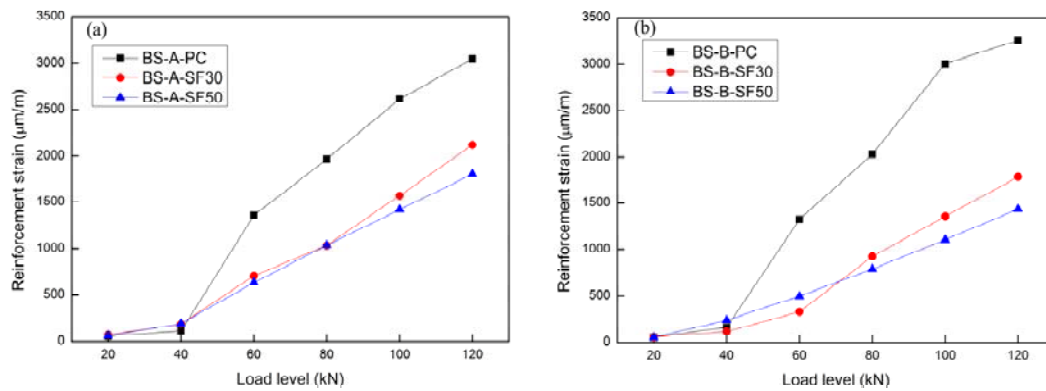
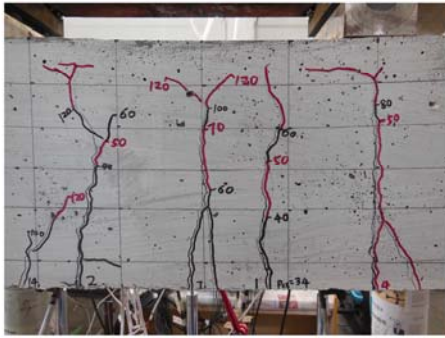
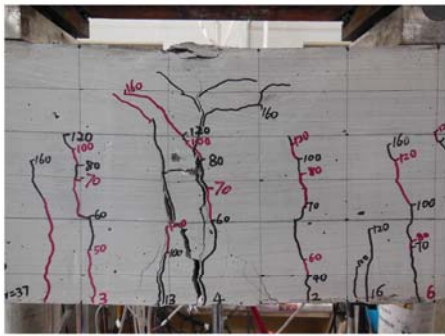


Fig. 7 Crack pattern for beam at the end of the test: (a) close up of the pure bending section; (b) complete look of the beam.



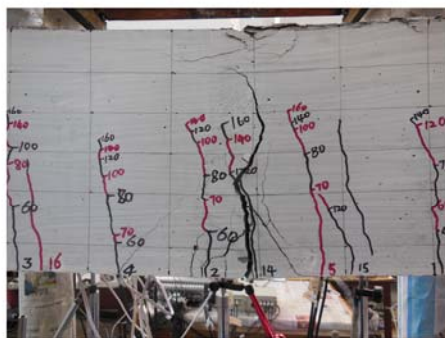
BS-A-PC



BS-A-SF50



BS-B-PC



BS-B-SF50

(a)

(b)

Fig. 8 Single fiber intersecting the crack plane.

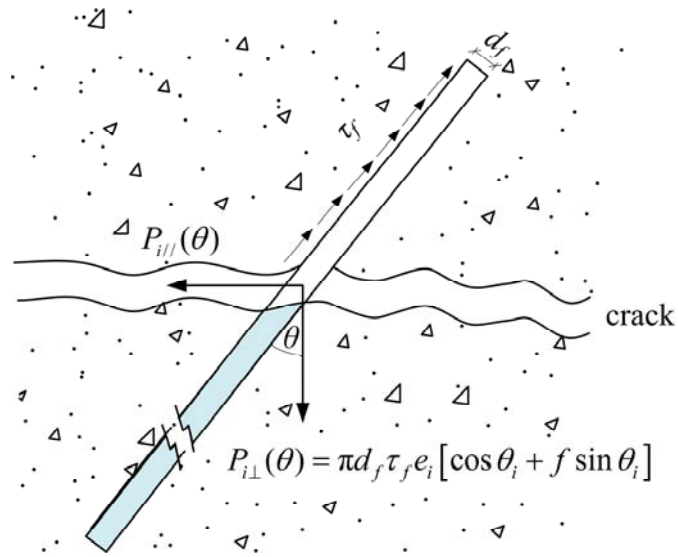


Fig. 9 Strain and stress distribution at cross section of steel fiber reinforced concrete beam at failure: (a) Cross-section; (b) Strain distribution; (c) Stress and force distribution.

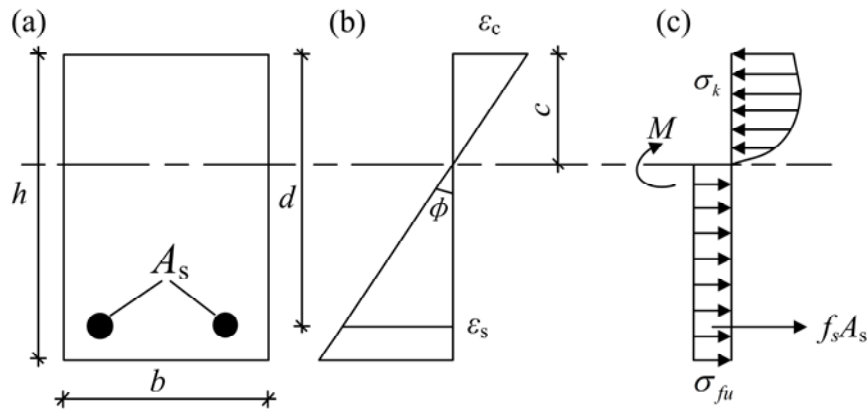


Fig. 10 Flow chart for analysis procedure of the suggested model.

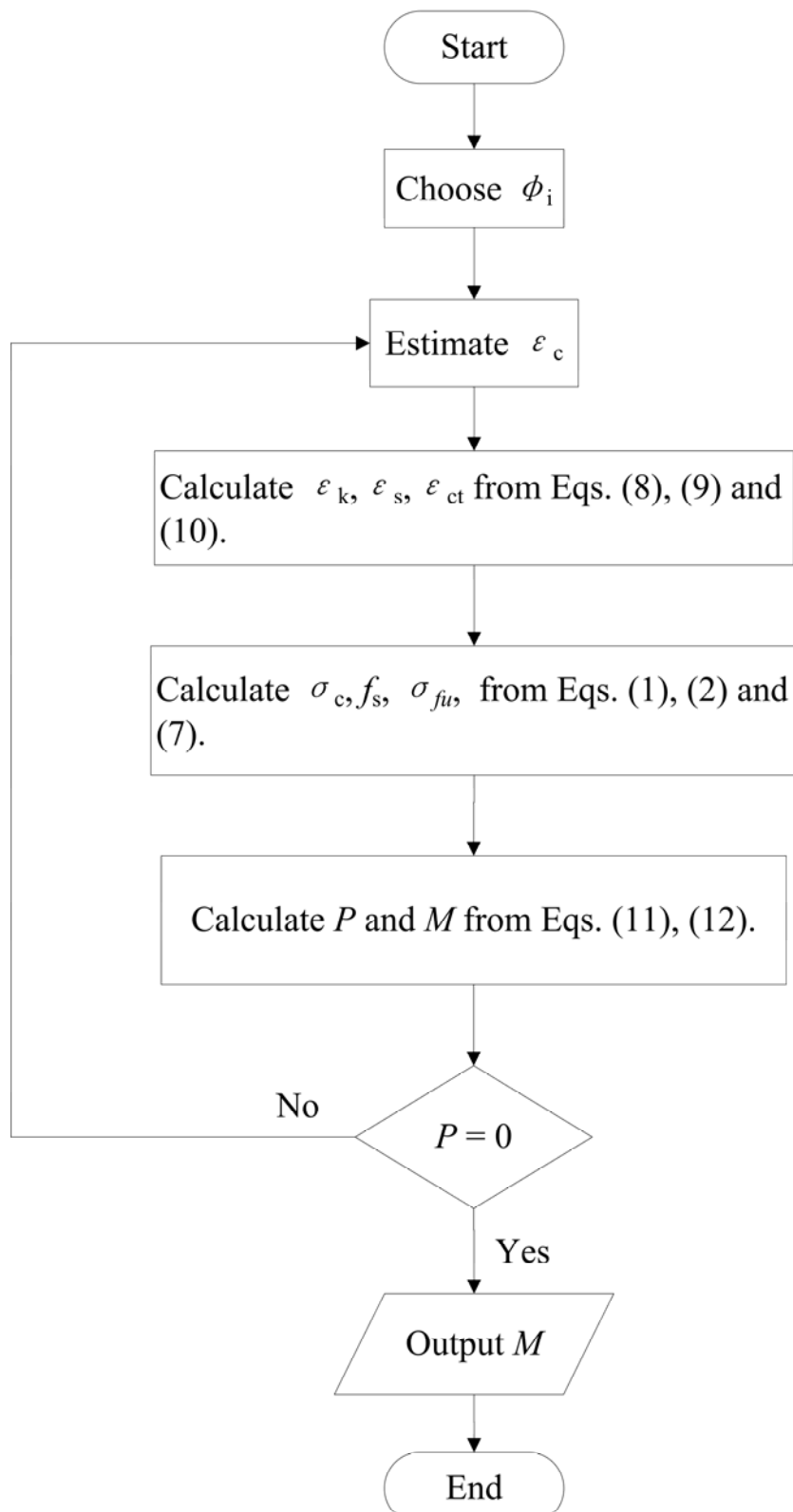


Fig. 11 Simplified stress-crack opening constitutive laws: a) Rigid-plastic model, b) Linear model (continuous and dashed lines refer to softening and hardening post-cracking behaviour, respectively).

